Influence of coal stress sensitivity on the desorption production characteristics and residual CH_4 distribution of thin multi-layered coal seams

Jianlong Xiong[1,2], Zhijun Zhang[2*], Qian Wang[1], Jian Shen[1], Paul W.J. Glover[3], Piroska Lorinczi[3], Jun Zhang[2], Siliang Zheng[4]

[1] *Key Laboratory of Coalbed CH4 Resources and Reservoir Formation Process, Ministry of Education, China University of Mining and Technology, Xuzhou, Jiangsu, 221008, China*
[2] *Sichuan Institute of Energetical and Geological Survey, Chengdu, 610072, China*
[3] *School of Earth and Environment, University of Leeds, Leeds, LS2 9JT, UK*
[4] *Sichuan Guxu Coalfield Development Co., Ltd*
*Corresponding author, Zhang Zhijun, cugzhijun@163.com

Abstract: Multi-layer co-development technology can significantly enhance the efficiency of coalbed methane (CBM) production in multi-layer thin coal seams. When facing multiple coal seams with low permeability and large differences in permeability between layers, investigating the impact of permeability and its stress sensitivity on the desorption and production patterns of methane (CH_4) is fundamental to the implementation of multi-layer co-development techniques. Permeability stress sensitivity tests on coal cores, CH_4 desorption production experiments, and quantitative analysis of CH_4 distribution in coal were conducted on coal samples with varying permeabilities in order to identify an optimal pressure drawdown approach that mitigates the adverse effects of permeability differences on multi-layer co-development. Experimental findings indicate that a significant shift in permeability ratios among coal seams is observed, from 1:18.9:5.4 to 1:43.1:10.8, which exacerbates interlayer differences, occurs as reservoir pressure decreases to the abandonment. The linear pressure decline method is found to be effective in enhancing CH_4 recovery, particularly in low-permeability coal, with a high recovery rate of 71.6%. This method outperforms both stepwise and direct pressure decline methods, which achieve recovery rates of 67.5% and 54.7%, respectively. The study also reveals that high-permeability coal exhibits 4.8~9.5%% higher CH_4 recovery rates than that of low-permeability coal with linear decrease in pressure. The high-permeability coal also reaches the peak CH_4 production rate earlier and maintain it for a longer period. The higher adsorbed CH_4 recovery rates and more uniform distribution of residual adsorbed CH_4 in high-permeability coal, suggesting that CH_4 in micropores is more readily desorbed. The study underscores the importance of reasonable bottom hole flowing pressure control for optimizing multi-layer co-development and provides a scientific basis for the effective development of CBM in the region.

Keywords: coalbed methane, multi-layer co-development, stress sensitivity, permeability, desorption, residual methane distribution

Introduction

The utilization of coalbed methane (CBM) has emerged as a significant component in the global energy landscape, offering a cleaner alternative to traditional fossil fuels[1-2]. The geological formations are particularly abundant in multiple thin coal seams which extend unbroken over a wide area and rich in methane (CH_4) content in the southern part of China's Sichuan Basin, presenting a substantial CBM resource potential[3].

Despite the abundance of CBM resources, the relatively small thickness of these coal seams poses a challenge to the productivity of individual CBM wells[4]. This limitation has necessitated the exploration of advanced extraction techniques, such as the practice of developing CBM from multiple layers of coal seams simultaneously or in a coordinated manner[5]. The multi-layer co-development approach holds the promise of enhancing the efficiency of CBM extraction by overcoming the constraints imposed by individual seam thickness[6].

However, the technical challenges associated with multi-layer co-development are not trivial. The heterogeneity in depth, pressure, and permeability across different coal seams can lead to interlayer interference, which is a critical factor affecting the overall performance of CBM recovery operations[7-8]. The Luban Mountain mining area is the study area, located in the southern Sichuan region. The coal seams in this mining area exhibit relatively small variations in depth and reservoir pressure, yet there is a significant disparity in permeability [9].

The permeability of coal reservoirs is highly sensitive to stress changes during the development process, a phenomenon known as stress sensitivity[10]. This sensitivity can exacerbate the interlayer interference issue, especially as the reservoir's pore pressure fluctuates with extraction. Understanding the stress sensitivity of coal seams and its impact on permeability is therefore crucial for optimizing CBM recovery strategies[11]. The control of bottom-hole flowing pressure is crucial as it dictates the variations in coal reservoir pressure in the process of CBM development [12-13]. A judicious management of these pressure changes can significantly alleviate the interlayer interference caused by permeability and its stress sensitivity, thus enhancing the efficiency of multi-layer co-development [14-15].

Previous studies have made significant progress in exploring the stress sensitivity of coal seams and the effects of permeability differences in multi-layer co-development reservoirs. The high-rank coal is characterized by a predominance of micro-pores and small-pores, high vitrinite content, and well-developed cleat-fractures, which exhibit strong stress-sensitive characteristics [16]. The rapid changes in stress can cause a significant stress-sensitive phenomenon in coals with low permeability[17], reducing CH_4 desorption efficiency by 30% to 80%, especially for CH_4 adsorbed in micropores, which have a higher residual saturation degree tested by the Low Field Nuclear Magnetic Resonance (LNMR)[18-19]. The recovery rate of multi-coalbed co-development decreases significantly with the increase in the initial permeability difference between coal seams[20-23], and as the pressure in the coalbed methane reservoir decreases, the interlayer contradiction becomes more pronounced[24-27].

However, the underlying patterns related to the differences in CH_4 desorption and production characteristics under various coal seam pressure decline methods have not been reported to date. Additionally, the distribution of CH_4 in coal before and after desorption is an important characteristic controlling the CH_4 desorption and production characteristics. Further monitoring is required to analyse the distribution changes of CH_4 in different states during the desorption and production process, to investigate the impact of permeability and stress sensitivity mechanisms on the effectiveness of multi-layer co-development.

Permeability stress sensitivity tests and CH_4 desorption production experiments were conducted on coal from the three main production coal seams of CBM in order to evaluate the feasibility of multi-layer coal seam mining in the Lubanshan mining area. The quantitative characterization of changes in CH_4 distributions in coal before and after desorption was carried out using LNMR technology. We also explored the stress sensitivity of permeability and its dynamic changes during the CBM development process. Furthermore, we assessed the impact of different pressure drawdown methods on CH_4 desorption production characteristics, and the distribution of residual CH_4, providing insights into the optimization of CBM extraction in complex, multi-layered coal seam environments.

Coal seam characteristics

The research target coalfield is the Luban Mountain mining area, located in the southern part of the Sichuan Basin in China. The mining area is divided into 8 mining areas (Figure 1). The Upper Permian Xuanwei Formation (P_2x) in the mining area has a coal-bearing stratigraphic system with

6 to 8 coal layers, showing the characteristic of multiple thin coal seams stacked and developed[28]. The depth of the coal layers ranges from 350 to 800 m. Among them, the 2#, 3# and 8# coal seams are stably occurring in the mining area. The main type of coal is anthracite, which is also the main productive seam for CBM production. However, the average permeability of the coal reservoir in the mining area is 0.95 md; this area being mainly characterized by low-permeability reservoirs. In addition, the single well production of CBM wells in the independent development process of a single coal seam is low, due to the small thickness of the coal seams, and hence the CBM development efficiency is poor. The No. 15 mining zone is located in the north-east corner of the mining area, and serves as a pilot area with two multi-branch cluster wells (X_1 and X_2) for CBM development, exploring multi-layer co-development to improve the efficiency of the CBM development.

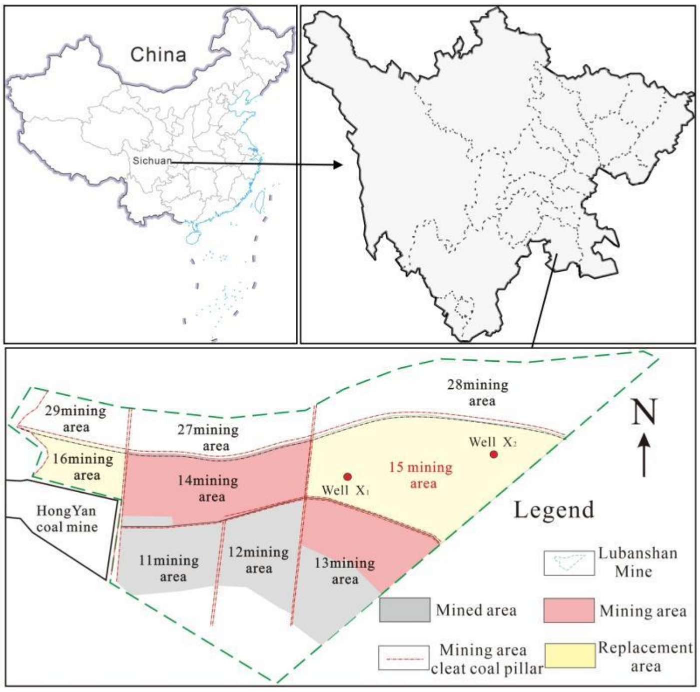

Figure 1. Location of Lubanshan Mining Area in Southern Sichuan, China.

The research target reservoir is composed of the 2#, 3#, and 8# coal seams in the 15th mining area of Lubanshan North Mine, which are located at a depth of 420 m to 550 m. The interlayer spacing is between 0.8 and 15.1 m, and the reservoir pressure gradient is between 9.5 kPa/m and 10.0 kPa/m, classifying it as a normally pressured reservoir with the reservoir pressure 4.11~5.45MPa. The reservoir possesses a relatively high energy level, which is conducive to longterm stable CH_4 production over a long period. The coal structure is primarily characterized by a primary-fragmented structure. The 2#, 3#, and 8# coal seams have thicknesses ranging between 0.74 m and 1.46 m, 0.74 m and 1.53 m, and 1.15 m and 4.47 m, respectively, with minimal variation in their thickness distribution. The temperatures of these three coal seams are stable at between 22.1℃ and 25.5℃. Additionally, the porosities of the 2#, 3#, and 8# coal seams are 3.62%~9.25%, 3.97%~10.12%, and 3.28%~8.87%, respectively.

However, there is a significant difference in the permeability of the three coal seams. The differences in reservoir permeability and stress sensitivity can lead to serious interlayer interference, which is an unfavourable factor for CH_4 multi-layer co-development. The 3# coal seam has the highest permeability, ranging from $0.093\times10^{-3}\mu m^2$~$7.86\times10^{-3}\mu m^2$, followed by the 8# coal seam at $0.053\times10^{-3}\mu m^2$~$6.77\times10^{-3}\mu m^2$, and the 2# coal seam has the lowest permeability, only $0.0085\times10^{-3}\mu m^2$~$2.18\times10^{-3}\mu m^2$. In the 15th mining area, the overall CH_4 content of the three coal seams is relatively high, with the CH_4 content of the 2#, 3#, and 8# coal seams being between 11.3 m^3 /t and 18.67 m^3 /t, 10.17 m^3 /t and 16.72 m^3 /t, and 15.08 m^3 /t and 23.05 m^3 /t, respectively. Specifically, the parameters of the three coal seams penetrated by the B_1 branch of well X_1 are shown in Table 1.

Overall, the 15th mining area, as a test area for multi-thin coal seam CH_4 co-development, has relatively small differences in depth, temperature, porosity, and gas content among its three main CH_4-producing coal seams. The difference in reservoir permeability is relatively large and may be a key factor affecting the effectiveness of multi-layer co-development. It is necessary to explore reasonable development parameters to mitigate the negative impact of permeability differences.

Table 1. The parameters of coal seams penetrated by the B_1 branch of well X_1.

Coal seam	Depth (m)	Thickness (m)	Reservoir pressure (MPa)	Temperature (℃)	Permeability (10^{-3} μm^2)	Porosity (%)	Gas content (m^3/t)
2 #	485.1	1.15	4.81	23.1	0.141	5.21	14.93
3 #	496.5	1.21	4.89	23.9	2.79	7.29	15.46
8 #	517.9	2.94	5.08	24.5	1.05	5.37	19.05

Methodology

Materials

Three large blocks of undeformed coal were extracted from each of the three coal seams to eliminate the potential impact of fractures on experimental results. The block coal samples were cut using wire cutting method to obtain multiple coal pillars. Among them, three cores (L2-1, L2-2, L2-3) with similar parameters were selected from the cylindrical samples of the 2# coal seam. Since the permeability of this coal seam is the smallest, its permeability sensitivity is expected to be the strongest. The selection of three cores corresponds to three different backpressure drop methods (confining pressure is fixed), to test the influence of pressure drop method on coal permeability stress sensitivity and the characteristics of CH_4 desorption production during the experiments. In addition, one sample was selected from each of the 3# and 8# coal seams (L3, L8). The permeabilities of the five selected core samples were close to the coal seams from which they came, the properties of the selected coal cores are shown in Tables 2.

Table 2. Basic parameters of the coal cores.

Coal number	Length (cm)	Diameter (cm)	Mass (g)	permeability (10^{-3} μm^2)	Porosity (%)	Backpressure drop method
L2-1	9.66	5.11	283.5	0.155	5.89	Linear descent
L2-2	9.63	5.09	281.59	0.151	5.92	Step descent
L2-3	9.48	5.08	279.4	0.152	5.95	Direct descent
L3	9.43	5.12	283.3	2.868	6.18	Linear descent
L8	9.88	5.11	287.1	0.825	6.5	Linear descent

Coal number	Source	$R_{o,max}$ (%)	Vitrinite (%)	Liptinite (%)	Inertinite (%)	Clay (%)	M_{ad} (%)	A_{ad} (%)	V_{daf} (%)	FC_{ad} (%)
L2-1		2.91	38.9	0.0	28.1	31.0	1.32	28.6	9.21	62.14
L2-2	2 # coal	2.92	37.6	0.0	28.9	30.5	1.28	29.47	9.38	61.22
L2-3		2.92	38.7	0.0	29.3	31.2	1.26	29.86	9.44	60.79
L3	3 # coal	2.89	53.0	0.0	23.0	22.0	1.16	23.86	9.05	67.08
L8	8 # coal	2.95	46.3	0.0	29.9	22.6	1.25	30.11	8.43	61.46

The scraps left over from the cutting process of the coal pillars were selected and processed into cubes with a side length of 3 cm. The CH_4 adsorption tests were carried out on these cube samples to test the ability of dry coal to adsorb CH_4. The adsorption time is about 2 to 4 days during the test, until the rate of CH_4 adsorption by the coal block decreases to 0.1 ml/h, allowing for the maximum possible adsorption of CH_4 within the coal. This duration is necessary to achieve a significant amount of CH_4 adsorbed onto the coal block, as the process is slower compared to the adsorption onto powdered coal. The results are shown in Figure 2. The brine used in the experiment was prepared in the laboratory according to the formation water data, the main cations were Ca^{2+}, Na^+, K^+, and Mg^{2+}, the main anions were Cl^-, and HCO_3^-, the formation water salinity was 2500 mg/L, and the water type was calcium chloride type. The methane concentration is 99.99%.

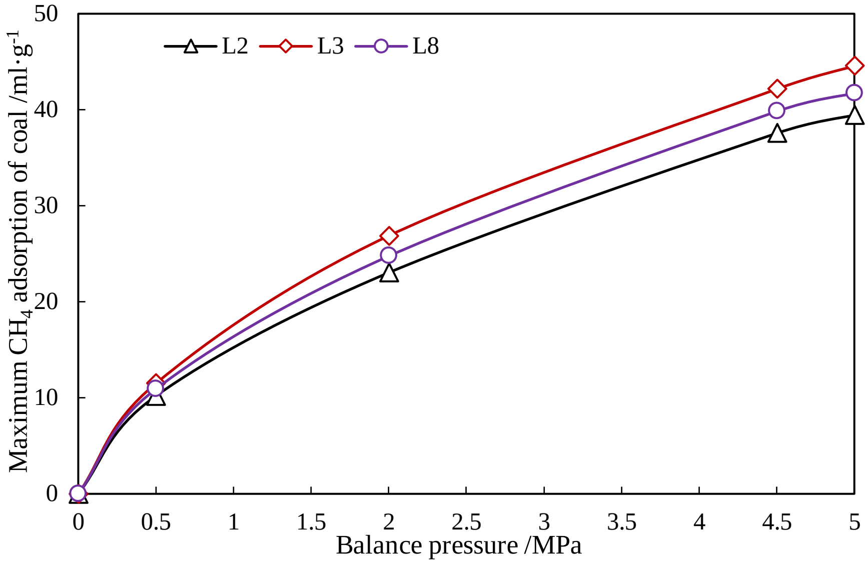

Figure 2. The CH_4 adsorption capacity of coal block samples at different equilibrium pressures at 25℃ without confining pressure.

Experimental apparatus and procedure

The experimental apparatus is composed predominantly of a displacement system, a fluid collection and metering system, a data acquisition system, and a low field nuclear magnetic resonance (LNMR) test system. A schematic diagram of the experimental apparatus is shown in Figure 3.

The LNMR technology can directly measure the CH_4 content in coal[29]. The essence of this method for studying CH_4 in coal is to use the relaxation characteristics of hydrogen-containing fluids in coal pores and cracks to analyse the different distributions of fluids in coal. The magnetic field interacts with the spin of the hydrogen nucleus, and the spin of the hydrogen nucleus reflects different amplitudes, also known as the relaxation time spectrum[30]. Its relaxation characteristics are generally expressed by relaxation time, which is divided into longitudinal relaxation time (T_1) and transverse relaxation time (T_2). The measurement of T_2 is simpler and faster, and the LNMR T_2 spectrum analysis technology is adopted. The pore size of coal is positively linearly related to the relaxation time, and hence the variations of the abscissa relaxation time of the nuclear magnetic resonance T_2 spectrum can be used to characterize the change of CH_4 distribution in coal pores[31].

The LNMR instrument used in tests is MesoMR23-060H-I, which has a resonant frequency of 21.3 MHz, and a magnetic field strength of 0.5 T. The core holder used in the experiment is customized to suit the LNMR tests, the confining pressure system range is 0 MPa to 25 MPa, and the temperature control system range is 5°C to 80°C. The CH_4 adsorption and desorption tests can be performed at different gas pressures. Since there are hydrogen atoms in both CH_4 and water during the experiment, to obtain the signal of hydrogen atoms in CH_4 and shield the signal of hydrogen atoms in brine during LNMR testing, deuterium water is used to prepare brine[32-33].

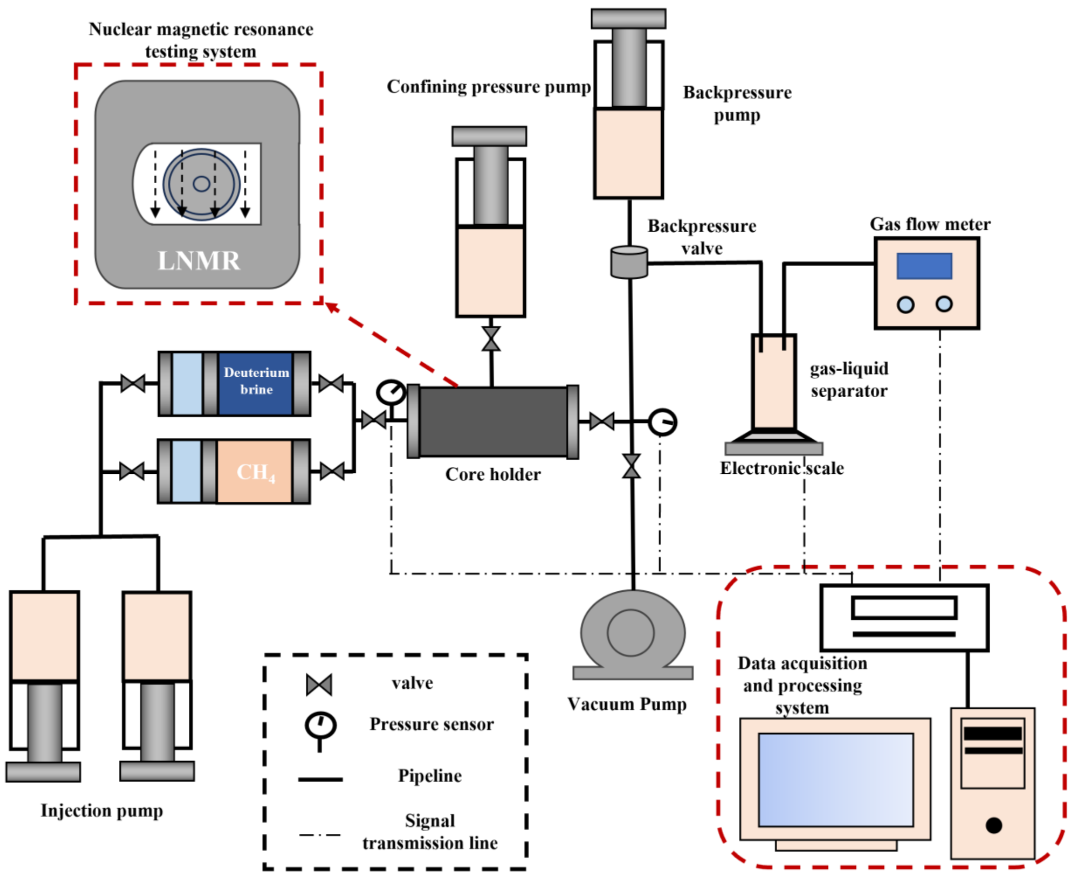

Figure 3. Experimental device for CH_4 adsorption and desorption with overburden pressure.

The experimental measurement of the adsorption and drainage process of CH_4 in coal consists of 4 steps:

① A permeability stress sensitivity test of the coal cores was carried out by using a helium porosity and permeability instrument, that is, the permeability of the coal core at different pressures was tested at a confining pressure of 6 MPa and 25°C. The helium pressure gradually dropped from 5 MPa (original reservoir pressure) to 0.5 MPa (residual pressure) during the tests.

② The transfer tanks were then filled with deuterium brine and CH_4. The core holders were placed in the LNMR testing equipment, with the laboratory temperature set to 25°C. The dry coal core was scanned by nuclear magnetic resonance to obtain the T_2 spectrum as the baseline reference line.

③ The confining pressure was set to 6 MPa. The CH_4 was injected into the coal core using an injection pump after the coal core was evacuated by a vacuum pump. During this process, the fluid pressure in the coal core was maintained at 4.5 MPa through the back pressure valve and the back pressure pump, and the CH_4 saturation time was 3 - 5 days. Subsequently, the back pressure was set to 5 MPa, and 3 PV (pore volume) of deuterium brine was injected at 2 ml/min to displace the free CH_4 in the coal core. At this time, the critical desorption pressure of CH_4 in the experimental coal was 4.5 MPa, while the fluid pressure in the pores was 5 MPa. The injected and produced CH_4 and water were recorded during this process, and the results are shown in Table 3 (The amount of CH_4 adsorbed by block coal with confining pressure is only 55.1% to 63.9% of that adsorbed by block coal without confining pressure under a balanced pressure of 5 MPa). The coal core was tested by nuclear magnetic resonance again to obtain the T_2 spectrum of saturated CH_4 in the coal.

④ The valve at the injection end of the core holder was closed, and three backpressure reduction drop modes were set (Figure 4) to carry out the desorption and drainage process of CH_4 and water, and the variations of CH_4 production rate over time was recorded. The drainage stage ends when the CH_4 production rate was less than 1 ml/h (the lower limit of effective gas production rate) for L2-1, L2-2, L2-3. The desorption drainage process for L2-1, L3 and L8 remained the same (200 h), since their backpressure decreased in the same way. Then the coal core was tested with LNMR again to obtain the T_2 spectrum of residual CH_4.

Please note that the apparatus separates and measures methane production and production rate allowing plots of methane production rate to be plotted as a function of desorption and production time.

Table 3. CH_4 adsorption without confining pressure in adsorption tests and CH_4 adsorption with confining pressure during desorption experiment.

CH_4 adsorption		CH_4 adsorption without confining pressure, ml/g			CH_4 adsorption with confining pressure of 6MPa, ml/g			R		
Balanced pressure, MPa		4.5	5	0.5	4.5	5	0.5	4.5	5	0.5
Coal number	L2-1	37.6	39.4	10.2	26.4	23.1	6.6	70.2	56.6	61.8
	L2-2				26.6	23.1	7.5	70.7	56.6	70.6
	L2-3				26.1	22.9	10.4	69.4	55.1	91.1
	L3	42.2	44.6	10.9	31.9	28.5	5.4	75.6	63.9	49.5
	L8	39.8	41.7	11.5	28.5	25.82	6.1	71.6	61.9	53.1

Notes: 4.5 MPa is the CH_4 saturation pressure, 5 MPa is the fluid pressure in the pores of pressurized coal after brine flooding, 0.5 MPa is the residual pressure after the experiment, and the R value is the ratio of the volume of CH_4 adsorbed in coal with confining pressure to the CH_4 adsorption volume without confining pressure during the experiment.

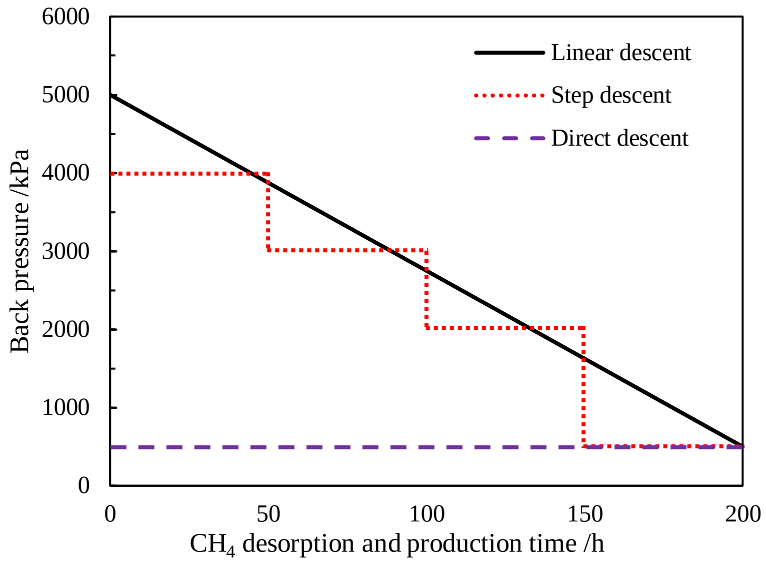

Figure 4. The backpressure drop pattern of coal core during desorption experiment.

Results and discussion

Coal permeability sensitivity

Permeability tests using helium gas were conducted at various gas pressure conditions to examine the permeability changes in different thin coal seams during the process of CBM multi-layer co-development. The results are illustrated in Figure 5, showing the permeability of coal core samples measured at a constant confining pressure of 6 MPa. The permeability of the coal core shows a decreasing trend as the helium gas pressure is reduced during the testing process. This trend is consistent across coal core samples with varying permeabilities. The trend is less steep at lower gas pressures, specifically between 0.5 and 4 MPa, the decrease in permeability becomes more significant at higher pressures, ranging from 4 to 5 MPa.

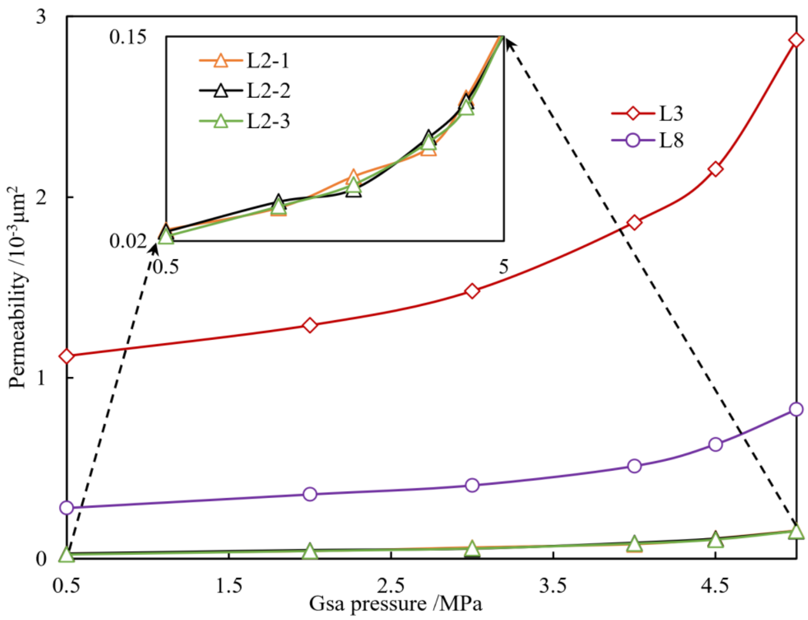

Figure 5. Permeability stress sensitivity of coal samples at 25℃.

The permeability sharply decreases due to the initial high helium gas pressure within the core pores, which leads to a smaller effective stress applied to the core. As the effective stress increases from 1 MPa to 2 MPa, the coal sample is compacted significantly, compressing the pores and fractures. This compression reduces the diameter of the effective pores and gas seepage pathways, resulting in a notable reduction in permeability. The coal sample's permeability gradually becomes more moderate. This is because, the volume of pores and fractures in the coal body is further compressed, as the test pressure decreases and the effective stress continues to increase. The compressive effect on pores and seepage pathways gradually diminishes when the effective stress reaches 4 MPa, leading to the diameter of the effective pores and seepage pathways tending to stabilize[34]. The permeability-gas pressure curve from the gas permeability test generally exhibits an exponential trend (Equation 1). The test data have been curve-fitted, and the fitting parameters for the coal sample permeability and gas pressure are shown in Table 4.

$$k = a \times e^{b\times(6-p)} \tag{1}$$

where k is permeability, $10^{-3}\mu m^2$, a, b are fitting coefficients, p is gas pressure, MPa.

Table 4. The fitting formula for the coal sample permeability and gas pressure.

Coal number	Fitting formula	R^2
L2-1	k=0.2312e$^{-0.4597(6-p)}$	0.966
L2-2	k=0.2253e$^{-0.4501(6-p)}$	0.976
L2-3	k=0.2283e$^{-0.4662(6-p)}$	0.975
L3	k=3.5887e$^{-0.2173(6-p)}$	0.943
L8	k=0.9921e$^{-0.2713(6-p)}$	0.938

It is evident that the value of “*a*” determines the overall level of the rock's permeability in the fitting formula (it represents the rock's initial permeability at p = 6 MPa), while the value of “*b*” determines the decline or the extent of the decrease in the curve. Thus, the value of “*b*” can be regarded as the stress sensitivity coefficient of permeability, which is related to the initial permeability of the core. The relationship between “*a*”, “$|b|$”, and the initial permeability of the core is shown in Figure 6.

Different coal seams exhibit significant differences in the macerals (Table 2). The L3 coal seam has the highest content of vitrinite, while the L2 coal seam has the lowest, and both the L3 and L8 coal seams have lower clay mineral content compared to the L2 coal seam. There is a correlation between the content of vitrinite and the initial permeability of the coal, which is attributed to the development of micro-fractures within the vitrinite, leading to higher permeability. Clay minerals, as pore-throat plugging materials, have a negative impact on coal permeability[16,35]. The micro-fractures within the vitrinite close under the influence of stress, resulting in the greatest decrease in permeability for the L3 coal. The deformation of clay minerals under stress has a very significant effect on the connectivity of the pore-throat in low-permeability coal, hence the high clay content L2 coal experiences a permeability loss of 86.7%, demonstrating a strong stress sensitivity.

In the process of co-development of CBM in multi-layer coal seams, variations in reservoir pressure (bottom hole flowing pressure) induce considerable differences in the permeability changes among different layers. The initial permeability ratio of coal L2, L3, and L8, which was 1:18.9:5.4, has shifted to 1:43.1:10.8, with the pressure decreasing from 5 MPa to 0.5 MPa, the disparity in interlayer permeability significantly increases. This phenomenon is detrimental to the efficient production of CH_4 in multi-layer co-development, potentially reducing the final recovery rate of CH_4[22-24,26]. Therefore, it is necessary to explore a reasonable bottom hole flowing pressure drop method during the multi-layer co-development process to minimize the impact of interlayer permeability differences and stress sensitivity differences on CH_4 production [36-37].

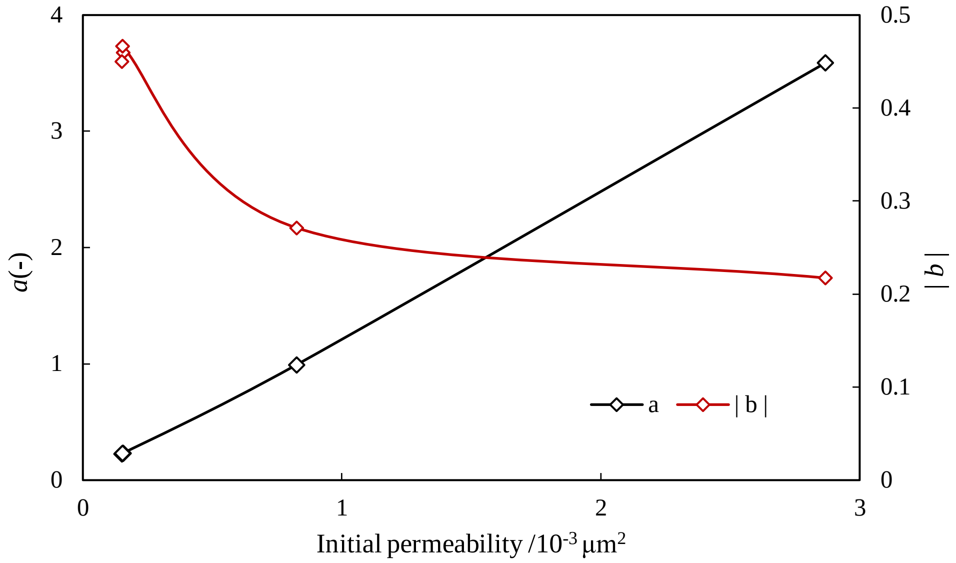

Figure 6. The initial permeability of the coal core and the fitting parameters "*a*" and "|*b*|".

CH_4 desorption and production characteristics

The production characteristics of CH_4 from coal core samples with similar properties in the most stress-sensitive coal seam L2 (L2-1, L2-2, L2-3) are shown in Figure 7, and Table 5. These samples were subjected to desorption experiments under the same conditions, but with different back pressure drop methods, which are commonly used in pressure control during the actual CH_4 production process. The bottom hole flowing pressure drop modes are categorized into three types: linear descent to abandonment pressure (0.5 MPa), stepwise descent, and direct reduction to abandonment pressure.

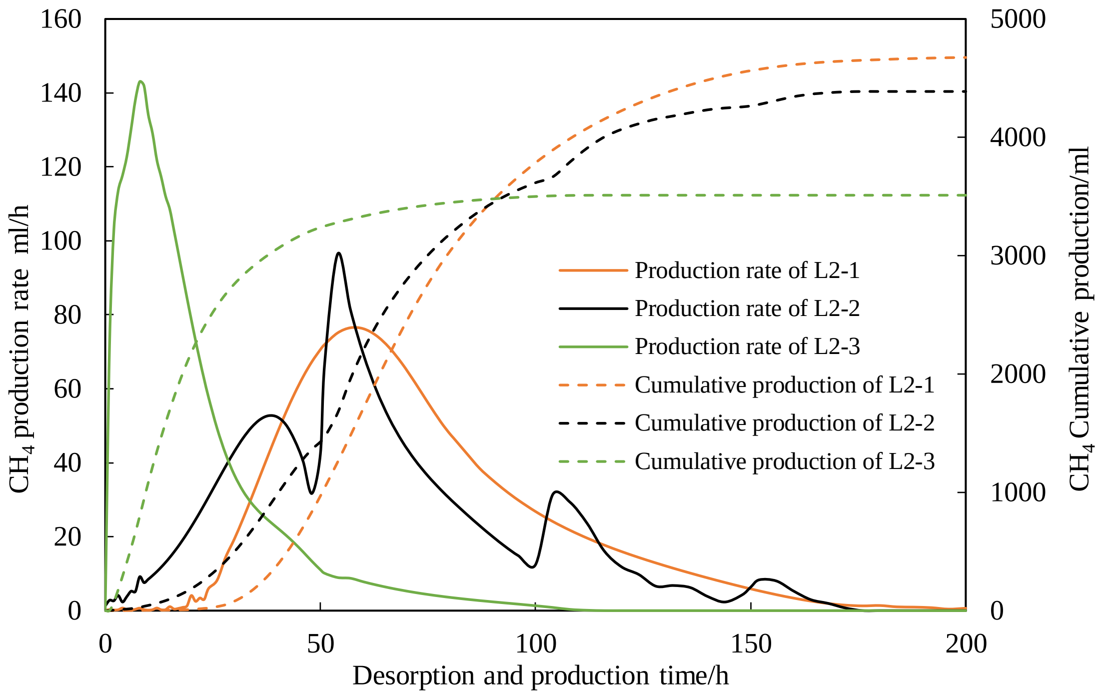

Figure 7. The production characteristics of CH_4 in coal core samples L2-1(linear descent), L2-2(stepwise descent), L2-3(direct descent).

Table 5. The production parameters of CH_4 in coal core samples L2-1, L2-2, L2-3.

Coal number	Backpressure drop method	Desorption and production time (h)	Total CH_4 recovery rate (%)	Desorption and production efficiency (%/h)
L2-1	Linear descent	200	71.6	0.358
L2-2	Step descent	172	67.5	0.392
L2-3	Direct descent	104	54.7	0.526
L3	Linear descent	200 (gas production rate still >1ml/h)	81.1	0.406
L8			76.4	0.382

A few bubbles accompany the brine in L2-1 with the linear decrease of pressure, when the back pressure is above 4.5 MPa (the critical desorption pressure of CH_4 set in the experiment), this indicates that in the process of brine displacement gas, the free CH_4 in the coal is not completely displaced. When the back pressure falls below 4.5 MPa, many bubbles begin to be produced. At this time, both brine and gas are produced simultaneously, and the gas production rate fluctuates, indicating that it is in the phase of simultaneous gas and water production[38]. The gas production rate begins to rise rapidly after 24 hours of desorption, and the fluctuation phenomenon disappears. The gas production rate reaches its maximum at 60 hours. Subsequently, the gas production rate begins to decline, but the rate of decline slows down over time. The gas production in the first 100 hours accounts for 81% of the total gas production, and the gas production in the last 50 hours accounts for 2.4% of the total. This production curve is basically consistent with the typical production curve of CBM wells in coal mines[39].

The first 50 hours represent the first decline step (4 MPa) for L2-2 with back pressure stepwise decline. It is also a phase of two-phase gas-water production in the first 9 hours, where the gas production rate fluctuates but rapidly increases, reaching the first peak in gas production at 38 hours. The gas production rate sharply increases and reaches a new peak value during the second pressure decline step. There is a significant difference in the time for the gas production rate reaching the peak value in the first two steps. The main reason is that there is a large amount of water in the pores during the first step, which affects the desorption of CH_4, and the difference between the fluid pressure in the pores and the critical desorption pressure is relatively small. The gas production rate quickly drops after the second peak, exhibiting a similar downward trend to that of L2-1 during this time. Although the second peak is notably higher than that of L2-1, the rate of gas production following the peak is lower than that of L2-1.

Another peak of gas production rate appears at the third step of the decline at 100 hours in L2-2, although the peak is much lower than the first two peaks, it effectively slows down the trend of the gas production rate decline. The fourth step's corresponding peak has a limited effect on delaying the decline of the gas production rate. The gas production rate has already fallen below 1 ml/h at 176 hours, which is shorter than the effective production time of 200 hours for L2-1. The CH_4 production corresponding to the four pressure decline steps accounts for 32.5%, 49.9%, 14.8%, and 2.8% of the total production, respectively. The gas production from the first two steps before 100 hours accounts for 82.4% of the total, which is similar to L2-2. Moreover, the overall trend of the gas production rate curves over time for L2-1 and L2-2 is consistent, except that the curve for L2-2 is shifted to the left and exhibits four peaks generated at the back pressure transitions.

The sample L2-3, with back pressure directly reduced to the abandonment pressure (residual pressure), sees its gas production rate rapidly increasing to a peak at 8 hours. It then quickly declines, begins to decrease more gradually after 50 hours, and the gas production rate falls below 1 ml/h at 104 hours. The gas production in the first 50 hours constitutes 92.3% of the total gas production. The peak value for L2-3 is significantly higher than that of L2-1 and L2-2, and the effective production time is notably shorter.

The overall CH_4 recovery rates for the L2-1, L2-2 and L2-3 are 71.6%, 67.5%, and 54.7%, respectively. It can be observed that L2-1 has the highest CH_4 recovery rate, while L2-3 has the lowest, with a difference of 16.9%. The reason is that the back pressure (pore fluid pressure) of L2-1 is always higher than that of L2-3 during the desorption process, and the permeability of L2-1 is consistently higher, especially in the early stages of gas production. The difference in effective stress experienced by the core is the greatest at this time, which results in a shorter effective production time for L2-3. This is due to the compression of coal pores and throats or the loss of connectivity of throats, affecting the desorption and seepage of CH_4. L2-2 experiences a significant amount of time with effective stress that is lower than L2-1 but higher than L2-3 during the CH_4 desorption process. However, it is not much different from L2-1, and there are nearly 30 hours when its effective stress is even lower than that of L2-1. Therefore, although the desorption of CH_4 in L2-2 is also affected by stress sensitivity, the effect is not significantly different from that of L2-1.

The linear decrease in back pressure (bottom hole flowing pressure) is beneficial for the highly stress-sensitive coal L2, as it helps to mitigate the negative impact of strong stress sensitivity on the efficiency of CH_4 desorption and the final recovery rate [40-41]. Although the direct decrease in back pressure results in a lower total recovery rate but a shorter duration, the linear decrease achieves a higher total recovery rate but requires a longer duration. Moreover, in the first half of the production time, which includes the water drainage phase, more than 80% of the gas is produced. A comparison of the average time required to achieve a 1% CH_4 recovery rate is made to analyze the production efficiency of different pressure drop methods, as shown in Table 6. L2-3 has the highest production efficiency at 0.526%/h, but its overall recovery rate is too low. Additionally, the short effective production time can exacerbate the interlayer interference effect during multi-layer co-development.

The linear decrease in back pressure extends the effective production time and increases the overall recovery rate, which is beneficial for the desorption and production of CBM wells with strong stress sensitivity. Figure 8 illustrates the CH_4 desorption and production characteristics of coal cores with different permeabilities, L2-1, L3, and L8, with linear back pressure decline.

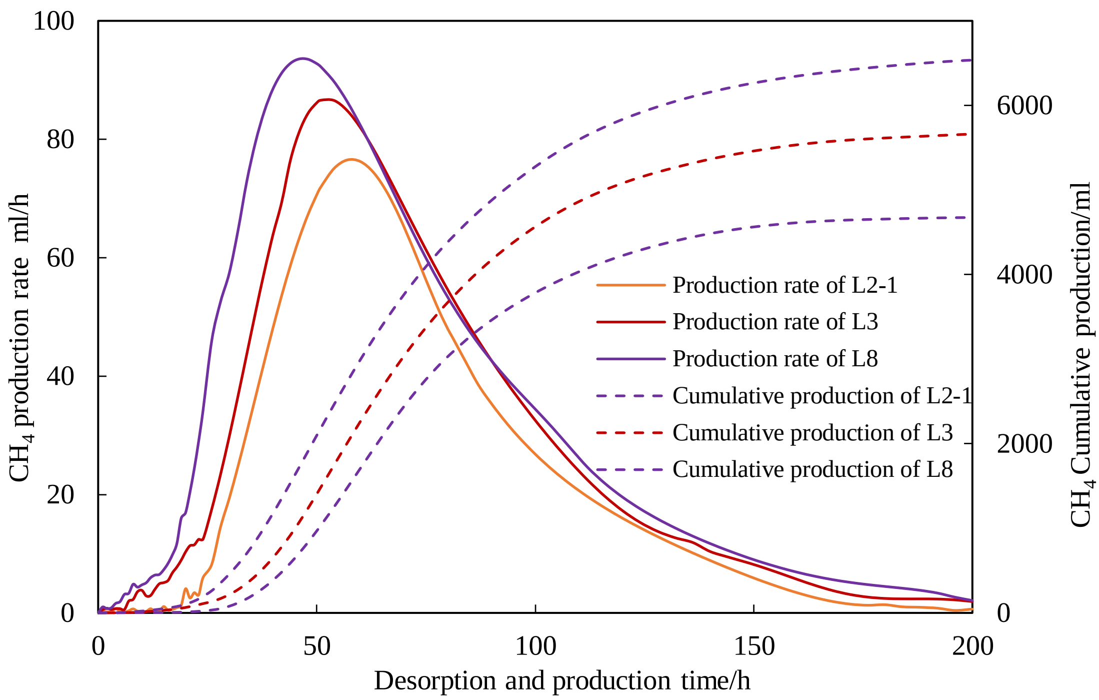

Figure 8. The production characteristics of CH_4 in coal core samples L2-1, L3 and L8 with linear back pressure decline.

The gas production rate curves of L3 and L8 follow the same trend as that of L2, but their times to first gas is earlier than L2, and the gas production rate of L3 and L8 reach the peak of gas production sooner than L2, with higher peak values. Throughout the process, the gas production rate of L3 and L8 is consistently higher than that of L2. The final CH_4 recovery rates for L3 and L8 is also higher than that of L2. Additionally, L3 and L8 still exhibit an effective gas production rate at 200 hours. In other words, core samples with higher permeability have an earlier time to first gas and reach peak gas production more quickly. They also maintain higher gas production rates and achieve higher recovery rates, with their effective production period being more extended[42]. The main reasons are that the core samples with high permeability have larger pore-throat sizes or better connectivity for drainage and gas production, smaller interfacial tensions between gas and water, less methane trapped in the pores by water, and higher efficiency in methane desorption and seepage[43-44].

Conversely, lower core permeability implies smaller pore-throat sizes, which means higher threshold pressures for gas-water two-phase flow and greater flow resistance, all of which are not conducive to CH_4 production. Especially under conditions of effective stress changes, the stress sensitivity of permeability can amplify the advantages of high-permeability core samples in terms of pore connectivity and fluid seepage. This means that the lower the permeability, the more significant the impact of stress sensitivity on the methane production process, making it even more challenging to CH_4 production compared to high-permeability cores. Although there are differences in CH_4 production characteristics among core samples of different permeabilities, considering the significant differences in initial permeability and stress sensitivity, the differences in gas production rates and final recovery rates are relatively small. This indicates that a linear decline method can effectively utilize the production potential of different coal seams in multi-layer co-development, achieving considerable development effects.

CH_4 distribution by LNMR T_2 Spectrum

Since the distribution of pore-throat sizes is the micro factor, which determines the desorption and production characteristics of CH_4 in coal, comparing the distribution of CH_4 in the coal pores before and after desorption we can indirectly understand the desorption and production characteristics of CH_4 in pores of different sizes. The T_2 spectrum of CH_4 distribution in the coal before and after desorption is shown in Figure 9 and Figure 10, respectively.

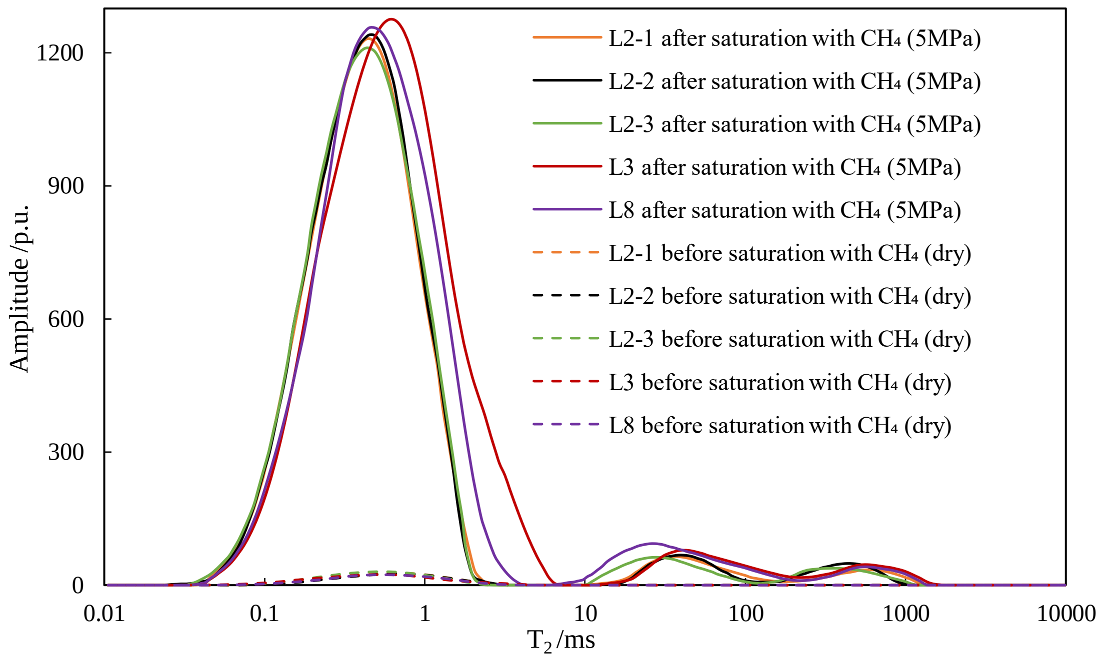

Figure 9. LNMR T_2 spectrum of dry coal core before the experiment and LNMR T_2 spectrum of saturation with CH_4 after brine injection at 5 MPa.

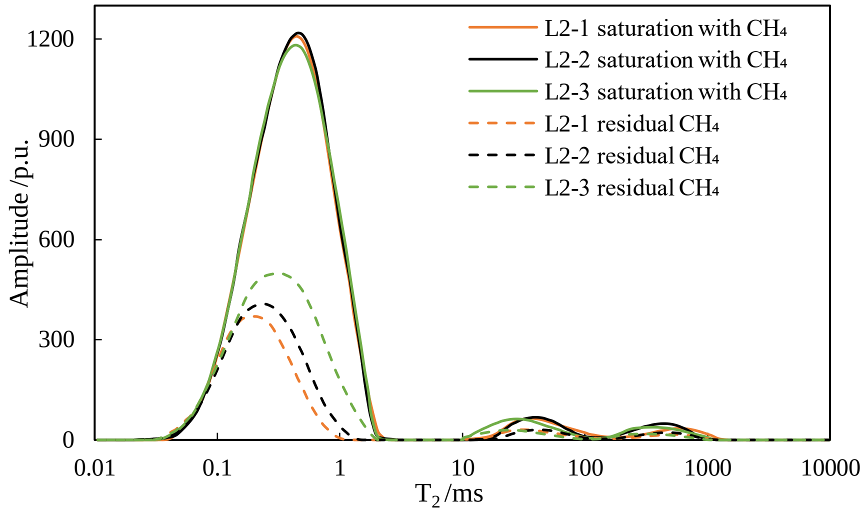

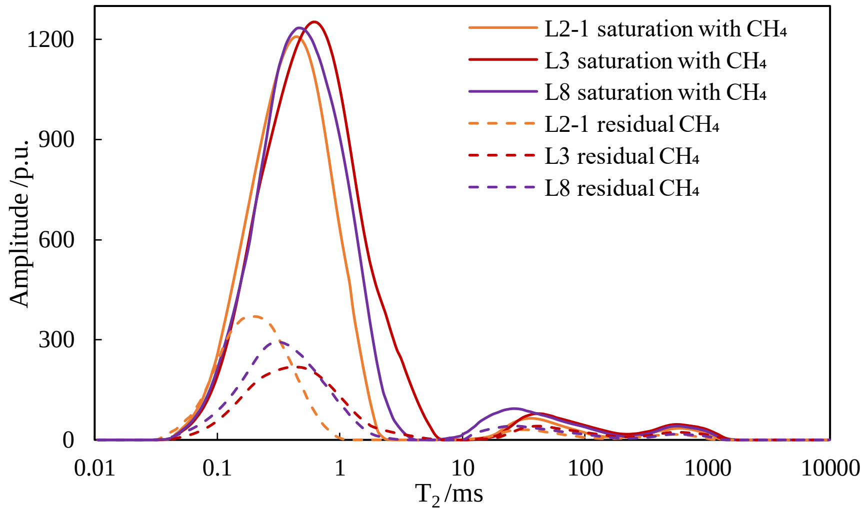

Figure 10. LNMR T_2 spectrum of saturation with CH_4 at 5 MPa and LNMR T_2 spectrum of residual CH_4.

Figure 9 includes the T_2 spectra of saturated CH_4 in 5 coal core samples under the condition of 4.5 MPa, and the T_2 spectra of CH_4 measured after being displaced by deuterated water at 5 MPa. In addition, the coal cores that were dried and not saturated with CH_4 and deuterated water were also tested by NMR, and their T_2 spectra served as the baseline. Figure 10 shows the distribution of initially saturated CH_4 and the residual CH_4 after desorption, corrected based on the baseline T_2 spectra of the dried core. It is generally believed that after CH_4 is adsorbed and saturated in coal, the measured T_2 spectrum contains three characteristic peaks from left to right, which are the adsorbed CH_4 peak, the free CH_4 peak, and the free CH_4 peak, corresponding to the signals of adsorbed CH_4, CH_4 constrained by porous media, and free CH_4 in coal, respectively[45]. The horizontal coordinates of the three peaks are located at 0.01 ms to about 7.31 ms, 9.82 ms to about 190.91 ms, and 204.97 ms to about 1426.67 ms, respectively. Studies have shown that these three peaks approximately correspond to the micropores, mesopores, and macropores of coal [46]. However, it is worth noting that the T_2 thresholds that some may want to impose globally between the different pore scale ranges probably do not exist in any useful sense due to the complexity of the coal structure, which gives rise to a wide range of T_2 values for any given imposed characteristic pore scale. Consequently, the types of pores are distinguished based on the occurrence of CH_4[47].

The total area of the peaks in the T_2 spectrum should be proportional to the volume of saturated CH_4 in the coal. Based on the measurement of CH_4 volume during the saturation and desorption process in the experiment, and the statistical analysis of the T_2 spectrum peak areas, the corresponding relationship is shown in Figure 11. As expected, the size of the peaks in the figure is proportional to the volume of CH_4, showing a very good linear relationship, indicating that the measurement results of CH_4 volume during the experimental process are consistent with the results of the LNMR testing.

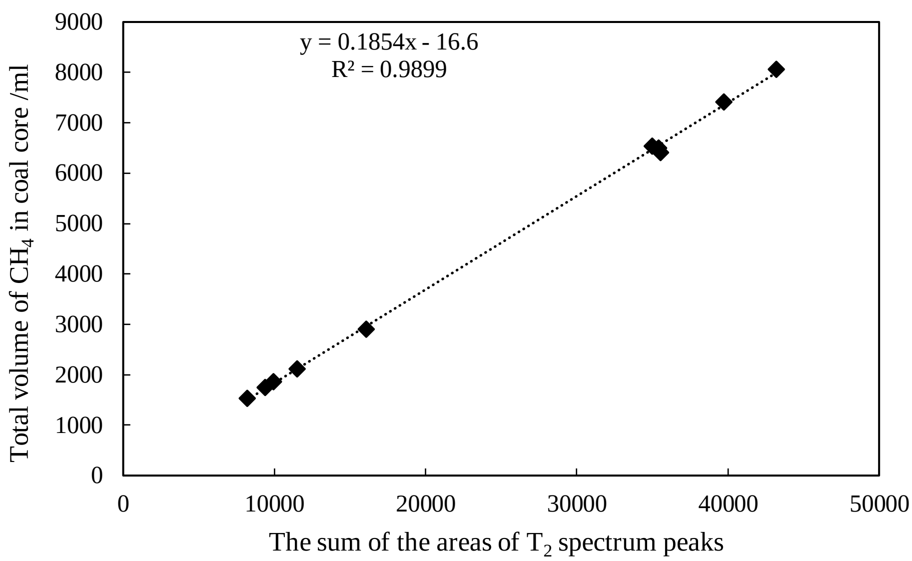

Figure 11. The relationship between the area of LNMR T_2 spectrum peaks and the volume of CH_4 in coal.

Based on the theory and experimental results, we can infer that the connectivity between adsorption pores and mesopores in the five coal samples is poor. This is indicated by the absence of CH_4 signals between the peaks corresponding to micropores and mesopores, suggesting that pores of these sizes are not well developed, especially in the core samples with lower permeability, such as L2-1, L2-2, L2-3. The pores corresponding to the 2.06 ms to about 16.91 ms T_2 spectrum are not well developed. There is also a possibility that pores of this size range are filled and occupied by water (water is difficult to enter micropores, but coexists with free CH_4 in mesopores and macropores, and during the water flooding process, the free gas is not completely displaced, and water, as a wetting phase, can fully fill the pore-throats of this size range), effectively severing the connection between micropores and mesopores. Since micropores adsorb a large amount of CH_4 (the vast majority of CH_4 in coal is in an adsorbed state [48-49]), and mesopores and macropores serve as permeable channels, the poor connectivity of micropore pathways results in CH_4 not being able to desorb, flow, and be produced smoothly even with a pressure drop. This is also the reason why the desorption of CH_4 in lump coal takes a longer time.

In contrast, there is a better connectivity between mesopores and macropores. Therefore, the connectivity between micropores and mesopores is the key factor that determines the efficiency of CH_4 desorption. Before the CH_4 desorption and production experiment, the distribution of saturated CH_4 in L2-1, L-2, and L-3 was similar, which also indicates that the distribution of core throat sizes is similar. The adsorption CH_4 peaks of coal L3 and L8 are wider than that of coal L2, with the main difference being that more CH_4 is adsorbed in the pores within the range of 1 ms to 5.9 ms in L3 and L8. Additionally, there is a greater amount of free CH_4 in the mesopores and macropores, which is why L3 and L8 see gas earlier than L2-1, L-2, and L-3 at the same pressure drop.

Figure 12 shows the recovery rates of CH_4 in different coal rocks calculated based on the recorded CH_4 production data and T_2 spectra. There is a significant difference in the distribution of residual adsorbed CH_4 for the L2-1, L2-2, L2-3 under different pressure drop conditions in Figure 6, and the corresponding recovery rates of adsorbed CH_4 also vary significantly, at 72.6%, 68.2%, and 54.9%, respectively. Specifically, the adsorption peak of residual CH_4 in L2-3 has the following characteristics: a large peak value and a wide peak width. This indicates that the desorption and production of CH_4 in the adsorption pores are subject to greater resistance under the condition of direct pressure drop. The stress sensitivity effect has a greater negative impact on the mass transfer of CH_4. The reason is still the strong stress sensitivity and a stronger water-locking effect that cuts off the gas flow channels[50].

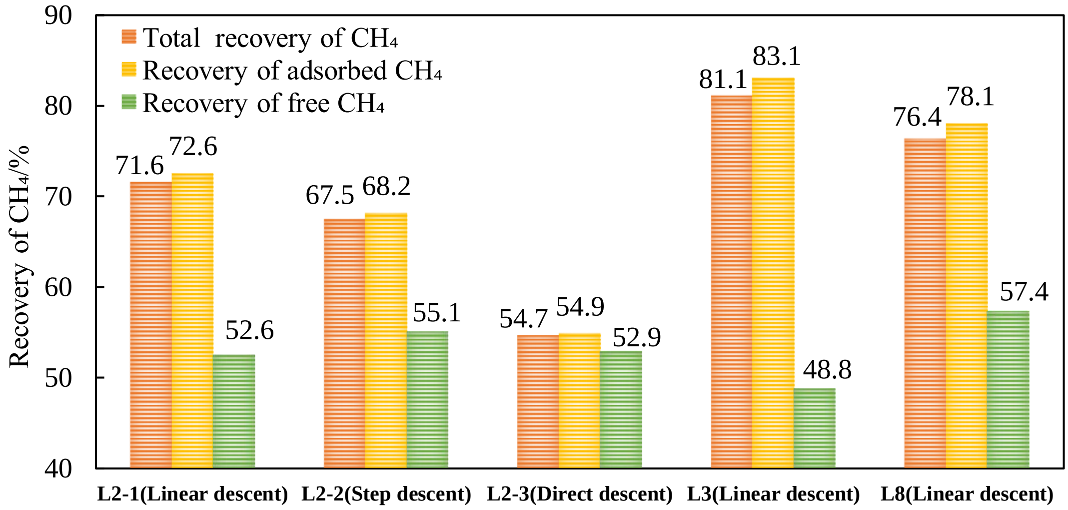

Figure 12. The recovery rates of CH_4 in different coal cores calculated based on the recorded CH_4 production data and T_2 spectra.

Additionally, it is worth noting that the T_2 values corresponding to the residual adsorbed CH_4 peak in L2-1, L2-2, and L2-3 are different (Table 6), and there is a certain amount of shift compared to the peak position of adsorbed CH_4 in the saturated state. The shift in the peak of residual adsorbed CH_4 in L2-1, L2-2, and L2-3 gradually decreases. The main reason for the shift in the adsorption peak in the T_2 spectrum is that the smaller the pore size, the more difficult it is for CH_4 to desorb and be produced, therefore, the residual amount of CH_4 in smaller pores is larger, and the corresponding recovery rate is lower. In contrast, more CH_4 is desorbed and produced in larger adsorption pores, resulting in a higher recovery rate. Among them, L2-3 has the smallest shift, indicating that there is a larger residual CH_4 in its larger adsorption pores during the experimental process. The difficulty of desorbing and producing CH_4 in the larger adsorption pores is also relatively greater, showing a weaker CH_4 production capability for L2-3.

Table 6. Peak position of CH_4 adsorption and adsorbed CH_4 recovery in micropore (T_2<0.1ms).

Coal number	Peak position for adsorption of CH_4 (T_2, ms)			Recovery of adsorbed CH_4 T_2<0.1 ms
	Saturation	Residue	Left offset	
L2-1	0.42	0.19	0.23	7.4%
L2-2	0.41	0.24	0.17	5.9%
L2-3	0.45	0.31	0.14	4.6%
L3	0.60	0.42	0.18	68.6%
L8	0.48	0.31	0.16	50.8%

Regardless of the type of pressure drop method, the CH_4 adsorbed in the pores corresponding to T_2 < 0.1 ms is the most stubborn residual CH_4, which is difficult to desorb. Promoting the desorption of CH_4 in some of the pores of the coal may require a longer time, or the fracturing and transformation of the pore fractures. The difficulty of improving the recovery rate of this adsorbed CH_4 through technical means is relatively high.

The differences in the distribution of residual free CH_4 among L2-1, L2-2, and L2-3 are relatively small, with corresponding recovery rates of 52.6%, 55.1%, and 52.9%, respectively. Their recovery rates are lower than that of adsorbed CH_4, especially for L2-1, where the difference reaches 20%. This is due to the desorption and flow of CH_4 in coal, where water in the pores is displaced, increasing the storage space for free CH_4. On the other hand, adsorbed CH_4 is desorbed from the adsorption pores and flows into the free pores to be produced. Although the original free CH_4 in the free pores is continuously produced, the CH_4 from the adsorption pores is continuously filling their space[51]. When CH_4 production stops, a large amount of free CH_4 still remains in the free pores. The increase in the free CH_4 space in the coal and the continuous replenishment of CH_4 in the free CH_4 space, however, is accompanied by a decrease in CH_4 pressure, which overall results in a relatively low recovery rate of free CH_4. This is not because free CH_4 is difficult to produce.

Although the same pressure drop method was used in the desorption production experiment for the core samples from three different coal layers, L2-1, L3, and L8, there is a significant difference in the distribution of residual CH_4 among the three cores. Firstly, there is a certain difference in the recovery rate of adsorbed CH_4, which are 72.6%, 83.1%, and 78.1%, respectively, indicating an increase with the rise in permeability. Moreover, the shift in the residual CH_4 adsorption peak is not necessarily such that the lower the recovery rate of adsorbed CH_4, the smaller the shift in the peak position in L2-1 and L3, L8, which is completely different from L2-1 and L2-2, L2-3. Instead, the higher the recovery rate of the core, the broader the residual CH_4 adsorption peak in the T_2 spectrum, indicating that in high-permeability cores, the distribution of residual CH_4 in adsorption pores of different sizes is more uniform, and the difference in CH_4 recovery rates among different adsorption pores is smaller. For example, the CH_4 recovery rate in the adsorption pores corresponding to $T_2 < 0.1$ ms in L3 and L8 reaches 68.6% and 50.8%, respectively, which is significantly higher than that in the low-permeability L2-1 (7.4%). This indicates that L3 and L8 exhibit better connectivity of pore throats, allowing for effective desorption and production of CH_4 from adsorption pores of various sizes, especially in smaller pores. Moreover, during the experimental process, after 200 hours, there is still an effective CH_4 production rate in L3 and L8, whereas, at this time, the effective production of CH_4 in L2-1 has already ceased. Therefore, high-permeability reservoirs not only have a high desorption and production efficiency, but also contain a large overall recoverable volume of methane, with significant production potential, and ultimately, a smaller amount of residual stubborn CH_4.

Additionally, the recovery rates of free CH_4 in L2-1, L3, and L8 are 52.6%, 48.8%, and 57.4%, respectively. There are differences, but these differences are relatively small. Among them, L3 has the lowest recovery rate of free CH_4, which may be due to the fact that during the production process of CH_4 desorption, water is more easily produced, thereby increasing the free space significantly.

Overall, as shown in Table 7, the proportion of CH_4 adsorbed on the five rock cores at CH_4 saturation conditions is nearly 94%. The change in the proportion of residual adsorbed CH_4 in L2-1, L2-2, and L2-3 is relatively small, decreasing by 0.3 ~ 3.5%. However, the proportion of residual adsorbed CH_4 decreases by 10.1% and 6.5% in L3 and L8, respectively, indicating that in high-permeability rock cores, adsorbed CH_4 is more likely to convert to the free state. Therefore, the strong stress sensitivity caused by direct pressure reduction hinders the transformation of adsorbed CH_4 to free CH_4 in the L2 coal seam (the desorption process). It also poses a significant resistance to the flow of CH_4, greatly reducing the efficiency of CH_4 production. Additionally, the desorption of CH_4 is less challenging in coal with high initial permeability, especially for CH_4 in smaller adsorption pores. The resistance to the flow and production of CH_4 is reduced, ultimately leading to a more desirable CH_4 recovery rate.

Table 7. Proportion of CH_4 adsorbed in cores.

Coal number	Saturation			Residue		
	Adsorption CH_4, ml	Free CH_4, ml	Adsorption proportion, %	Adsorption CH_4, ml	Free CH_4, ml	Adsorption proportion, %
L2-1	6179.5	352.7	94.6	1691.8	165.8	91.1
L2-2	6135.4	364	94.4	1950.1	162.1	92.3
L2-3	6046.7	365.5	94.3	2728.7	173.4	94
L3	7589.6	475.9	94.1	1284.9	244.8	84
L8	6827.2	585.6	92.1	1500.1	251.3	85.6

Ultimately, the overall recovery rates of CH_4, adsorbed CH_4, and free CH_4 are controlled within a 10% difference for the three coal cores L2-1, L3, and L8 at the condition of linear pressure decline. This is a relatively small and ideal interlayer discrepancy, especially considering the large initial permeability differences. Therefore, for the three coal seams in the study area, a method of linear backpressure decline can be adopted for multi-layer co-development of CBM.

Conclusions

The CH_4 desorption and production experiments investigated the impact of coal seam permeability stress sensitivity and the effects of pressure drawdown methods on CH_4 desorption characteristics and the distribution of residual CH_4. The specific conclusions are as follows,

1) The permeability ratio of the 2#, 3#, and 8# coal seams shifted significantly from the initial state of 1:18.9:5.4 to 1:43.1:10.8, when the reservoir pressure is reduced from 5 MPa to 0.5 MPa, indicating a pronounced increase in the interlayer permeability difference.

2) The recovery rates corresponding to the backpressure linear decline, stepwise decline, and direct decline to abandonment pressure were 71.6%, 67.5%, and 54.7%, respectively during the CH_4 desorption and production process in the 2# coal. The linear decline in backpressure can extend the effective production time of CH_4.

3) The CH_4 recovery rates for the high-permeability 3# and 8# coal are 9.5% and 4.8% higher than that of the 2# coal, respectively. They also reach the peak CH_4 production rate earlier and maintain it for a longer period.

4) The recovery rates of adsorbed CH_4 in the 2# coal under backpressure linear decline, stepwise decline, and direct decline conditions were 72.6%, 68.2%, and 54.9%, respectively. The desorption and production of CH_4 in the adsorption pores face greater resistance under the condition of direct pressure drop.

5) The distribution of residual adsorbed CH_4 in high-permeability coal is more uniform under the condition of linear backpressure decline, and the recovery rates of adsorbed CH_4 are 10.5% and 5.5% higher than in low-permeability coal. CH_4 in the micropores of high-permeability coal seams is more easily desorbed and produced.

In summary, a linear decline in backpressure can mitigate the negative impact of stress sensitivity on CH_4 desorption and production effects, which is beneficial for the co-development of CH_4 in coal seams with large initial permeability differences in the study area.

Acknowledgments

This research is supported by National Natural Science Foundation of China, “Cross-scale precipitation mode of asphaltene in ultra-deep sandstone reservoir during CO_2 flooding” (52104048), and “Geological Constraint mechanism and optimization of deep coal measures reservoirs activated by caving” (42272198).

References

[1] Liang W, Yan J, Zhang B, Hou D. Review on coal bed methane recovery theory and technology: recent progress and perspectives. Energy & Fuels, 2021, 35(6), 4633-4643.
[2] Mallick N, Prabu V. Energy analysis on Coalbed Methane (CBM) coupled power systems. Journal of CO_2 Utilization, 2017,19, 16-27.
[3] Bi C, Zhang J, Shan Y, Hu Z, Wang F, Chi H, Tang Y, Yuan Y, Liu Y. Geological characteristics and co-exploration and co-production methods of Upper Permian Longtan coal measure gas in Yangmeishu Syncline, Western Guizhou Province, China. China Geology, 2020, 3(1), 38-51.
[4] Ren J, Zhang L, Ren S, Lin J, Meng S, Ren G, Gentzis T. Multi-branched horizontal wells for coalbed methane production: Field performance and well structure analysis. International Journal of Coal Geology, 2014, 131, 52-64.
[5] Ziarani A, Aguilera R, Clarkson C. Investigating the effect of sorption time on coalbed methane recovery through numerical simulation. Fuel, 2011, 90(7), 2428-2444.
[6] Szott W. Słota-Valim M, Gołąbek A, Sowiżdżał K, Łętkowski P. Numerical studies of improved methane drainage technologies by stimulating coal seams in multi-seam mining layouts. International Journal of Rock Mechanics and Mining Sciences, 2018,108, 157-168.
[7] Moore T A. Coalbed methane: a review. International Journal of Coal Geology, 2012,101, 36-81.
[8] Chen Y, Luo J, Hu X, Yang Y, Wei C, Yan H. A new model for evaluating the compatibility of multi-coal seams and its application for coalbed methane recovery. Fuel, 2022, 317, 123464.
[9] Jia L, Peng S, Xu J, Yan F. Fluid response characteristics of multilayer superimposed CBM production under the different number of gas-producing layers condition. Journal of Natural Gas Science and Engineering, 2021, 89, 103858.
[10] Behnoudfar P, Asadi M B, Gholilou A, Zendehboudi S. A new model to conduct hydraulic fracture design in coalbed methane reservoirs by incorporating stress variations. Journal of Petroleum Science and Engineering, 2019,174, 1208-1222.
[11] Fang H, Li A, Sang S, Gu C, Yang J, Li L, Liu H, Xu H, Huang Y. Numerical analysis of permeability rebound and recovery evolution with THM multi-physical field models during CBM extraction in crushed soft coal with low permeability and its indicative significance to CO_2 geological sequestration. Energy, 2023, 262, p.125395.
[12] Kumar H, Mishra M K, Mishra S. Effect of Permeability and Geomechanical Properties on Coal Matrix During CBM Production-An Overview. Journal of Engineering Science & Technology Review, 2018,11(2).
[13] Xu H, Sang S, Yang J, Jin J, Hu Y, Liu H, Li J, Zhou X, Ren B. Selection of suitable engineering modes for CBM development in zones with multiple coalbeds: A case study in

western Guizhou Province, Southwest China. Journal of Natural Gas Science and Engineering, 2016,36, 1264-1275.
[14] Wang Z, Qin Y. Physical experiments of CBM coproduction: A case study in Laochang district, Yunnan province, China. Fuel, 2019, 239, 964-981.
[15] Clarkson C R, Bustin R M. Coalbed methane: current evaluation methods, future technical challenges. In SPE Unconventional Resources Conference/Gas Technology Symposium,2010, February, SPE-131791.
[16] Li S, Tang D, Pan Z, Xu H, Huang W. Characterization of the stress sensitivity of pores for different rank coals by nuclear magnetic resonance. Fuel ,2013, 111, 746-754.
[17] Wang L, Long Z, Qu Z, Song Y, Liu B. Effects of functional groups on supercritical CH_4 adsorption and desorption characteristics of tectonically deformed coals. Fuel, 2022,325, 124934.
[18] Quan F, Wei C, Zhang J, Feng S, Hao S, Lu G, Hu Y. Study on desorption and diffusion dynamics of coal reservoir through step-by-step depressurization simulation——an experimental simulation study based on LF-NMR technology. Journal of Natural Gas Science and Engineering, 2020, 75, 103149.
[19] Zhang J, Wei C, Ju W, Yan G, Lu G, Hou X, Kai Z. Stress sensitivity characterization and heterogeneous variation of the pore-fracture system in middle-high rank coals reservoir based on NMR experiments. Fuel,2019, 238, 331-344.
[20] Zhang X, Ranjith P G, Perera M S A, Ranathunga A S, Haque A. Gas transportation and enhanced coalbed methane recovery processes in deep coal seams: a review. Energy & Fuels, 2016,30(11), 8832-8849.
[21] Wang Z, Qin Y, Li T, Zhang X. A numerical investigation of gas flow behavior in two-layered coal seams considering interlayer interference and heterogeneity. International journal of mining science and technology, 2021, 31(4), 699-716.
[22] Zhang Y, Underschultz J, Langhi L, Mallants D, Strand J. Numerical modelling of coal seam depressurization during coal seam gas production and its effect on the geomechanical stability of faults and coal beds. International Journal of Coal Geology, 2018,195, 1-13.
[23] Zhao Y, Wang Z. Effect of interlayer heterogeneity on multi-seam coalbed methane production: A numerical study using a gray lattice Boltzmann model. Journal of Petroleum Science and Engineering, 2019,174, 940-947.
[24] Gouth F, Belushko I, Herwin H. Dynamic behavior of a multi-seamed coal seams gas reservoir in the Bowen Basin. In SPE Asia Pacific Oil and Gas Conference and Exhibition, 2014, pp. SPE-171538.
[25] Jiang W, Wu C, Wang Q, Xiao Z, Liu Y. Interlayer interference mechanism of multi-seam drainage in a CBM well: An example from Zhucang syncline. International Journal of Mining Science and Technology, 2016, 26(6), 1101-1108.
[26] Santiago V, Ribeiro A, Hurter S. Modelling the Contribution of Individual Seams to Coal Seam Gas Production. In SPE/AAPG/SEG Asia Pacific Unconventional Resources Technology Conference, 2019, November, p. D022S027R002, URTEC.
[27]Zhang X, Wu B, Connell L, Han Y, Jeffrey R. Hydraulic Fracturing Treatment of Low-Permeability Coal Seam Gas Reservoirs with Finely Layered Coals. In SPE Asia Pacific Oil and Gas Conference and Exhibition,p. D031S026R002). SPE,2018, October.
[28] Chen Y, Guo C, Dou W. The Resource Potential and the Prospect of Coal Bed Methane (CBM) In Western Guizhou And Eastern Yunnan of China. In World Petroleum Congress, 2005,

pp. WPC-18.
[29] Turakhanov A H, Shumskayte M Y, Ildyakov A V, Manakov A Y, Smirnov V G, Glinskikh V N, Duchkov A D. Formation of methane hydrate from water sorbed by anthracite: An investgation by low-field NMR relaxation. Fuel, 2020,262, p.116656.
[30] Li L, Liu D, Cai Y, Wang Y, Jia Q. Coal structure and its implications for coalbed methane exploitation: a review. Energy & Fuels, 2020,35(1), 86-110.
[31] Alexeev A D, Ulyanova E V, Starikov G P, Kovriga N N. Latent methane in fossil coals. Fuel, 2004,83(10), pp.1407-1411.
[32] Zheng S, Yao Y, Elsworth D, Liu D, Cai Y. Dynamic fluid interactions during CO_2-enhanced coalbed methane and CO_2 sequestration in coal seams. Part 1: CO_2–CH_4 interactions. Energy & Fuels, 2020,34(7), 8274-8282.
[33] Liu L, Yang M, Zhang X, Mao J, Chai P. LNMR experimental study on the influence of gas pressure on methane adsorption law of middle-rank coal. Journal of Natural Gas Science and Engineering, 2021,91, 103949.
[34] Danesh N N, Chen Z, Connell LD, Kizil M S, Pan Z, Aminossadati S M. Characterisation of creep in coal and its impact on permeability: an experimental study. International Journal of Coal Geology, 2017,173, pp.200-211.
[35] Meng Z, Li G. Experimental research on the permeability of high-rank coal under a varying stress and its influencing factors. Engineering Geology, 2013,162, 108-117.
[36] Wang Q, Shen J, Glover PW, Lorinczi P, Duncan I. Improving the Prediction of Production Loss in Heterogeneous Tight Gas Reservoirs Using Dynamic Threshold Pressure. Energy & Fuels, 2022, 36(19), 11991-12003.
[37] Chattaraj S, Upadhyay R, Mohanty D, Halder G, Kumar T. Evaluating production behaviour of CBM wells from Raniganj Coalfield through reservoir characterization under constrained field data conditions. Journal of Natural Gas Science and Engineering, 2021,92, p.103969.
[38] Seo S, Mastiani M, Hafez M, Kunkel G, Asfour CG, Garcia-Ocampo KI, Linares N, Saldana C, Yang K, Kim M. Injection of in-situ generated CO_2 microbubbles into deep saline aquifers for enhanced carbon sequestration. International Journal of Greenhouse Gas Control, 2019, 83, 256-264.
[39] Clarkson C R, Salmachi A. Rate-transient analysis of an undersaturated CBM reservoir in Australia: Accounting for effective permeability changes above and below desorption pressure. Journal of Natural Gas Science and Engineering, 2017,40, pp.51-60.
[40] Jamshidi M, Jessen K. Water production in enhanced coalbed methane operations. Journal of Petroleum Science and Engineering, 2012,92, pp.56-64.
[41] Wang Q, Zhu B, Shen J, Glover PW, Lorinczi P, Han H. Quantifying controls on threshold pressure during CO_2 injection in tight gas reservoir rocks. Energy & Fuels, 2022, 36(12), 6292-6304.
[42] Clarkson C R, Jordan C L, Gierhart R R, Seidle J P. Production data analysis of CBM wells. In SPE Rocky Mountain Petroleum Technology Conference/Low-Permeability Reservoirs Symposium, 2007, April, pp. SPE-107705.
[43] Arif M, Barifcani A, Lebedev M, Iglauer S. CO_2-wettability of low to high rank coal seams: Implications for carbon sequestration and enhanced methane recovery. Fuel, 2016,181, pp.680-689.
[44] Bustin A M M, Bustin R M, Moudrakovskim I L, Takeya S, Ripmeester J A. Formation of

methane clathrate hydrates in coal moisture: implications for coalbed methane resources and reservoir pressures. Energy & Fuels, 2016,30(1), 88-97.
[45] Zhao Y, Sun Y, Liu S, Wang K, Jiang Y. Pore structure characterization of coal by NMR cryoporometry. Fuel, 2017, 190, 359-369.
[46] Cai Y, Liu D, Pan Z, Yao Y, Li J, Qiu Y. Petrophysical characterization of Chinese coal cores with heat treatment by nuclear magnetic resonance. Fuel, 2013, 108, 292-302.
[47] Guang W, Zhang Z, Zhang L, Ranjith P G, Hao S, Liu X. Confinement effect on transport diffusivity of adsorbed CO_2–CH_4 mixture in coal nanopores for CO_2 sequestration and enhanced CH_4 recovery. Energy, 2023,278, 127929.
[48] Kędzior S. Methane contents and coal-rank variability in the Upper Silesian Coal Basin, Poland. International Journal of Coal Geology, 2015, 139, pp.152-164.
[49] Skoczylas N. Laboratory study of the phenomenon of methane and coal outburst. International Journal of Rock Mechanics and Mining Sciences, 2012, 55, pp.102-107.
[50] Cai Y, Zhai C, Yu X, Sun Y, Xu J, Zheng Y, Cong Y, Li Y, Chen A, Xu H, Wang S, Wu X. Quantitative characterization of water transport and wetting patterns in coal using LF-NMR and FTIR techniques. Fuel, 2023, 350, 128790.
[51] Alexeev A D, Feldman E P, Vasilenko T A. Methane desorption from a coal-bed. Fuel, 2007,86(16), pp.2574-2580.

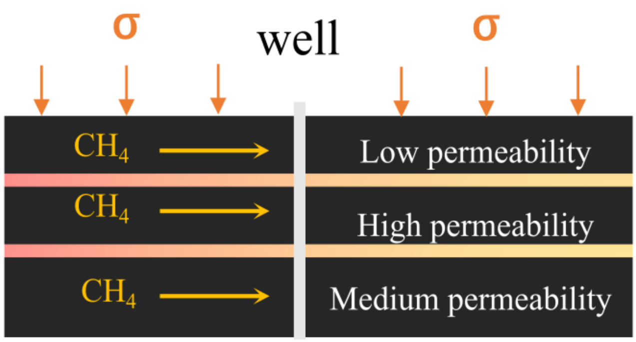

TOC graphic:Stress sensitivity in the multi-layer co-development process of thin coal seams with different permeabilities.